Dynamic disorder in acenaphthylene. A solid state deuterium NMR study

Thomas Bräuniger,[a] Raphy Poupko,[a] Herbert Zimmermann[b] and Zeev Luz[a]

[a] *The Weizmann Institute of Science, Rehovot 71600, Israel*
[b] *Max-Planck-Institut für Medizinische Forschung, AG Molekülkristalle, 69120 Heidelberg, Germany*

The dynamic disorder in solid acenaphthylene has been studied by deuterium NMR spectroscopy of deuteriated powder samples. The spectra exhibit lineshape and relaxation discontinuities in the transitions from Phase III, through Phase II, to Phase I (the latter being stable above 127 K). A detailed analysis of the lineshape and T_1 relaxation in Phase I is presented. The results show the occurrence of two distinct equally populated, dynamic sites. The molecules in both sites undergo planar reorientation, but with different Arrhenius kinetic parameters: $k_1^0 = 1.5 \times 10^{12}$ s^{-1}, $\Delta E_1 = 10.2$ kJ mol^{-1}; $k_2^0 = 4.8 \times 10^{12}$ s^{-1} and $\Delta E_2 = 18.3$ kJ mol^{-1}. The results are consistent with earlier proton second moment and relaxation measurements and provide additional information on the nature of the motion. It is argued that the subspectra with the slower and faster motions are associated, respectively, with the (A,B) and C layers in the crystal.

Introduction

Many compounds which crystallize as regular lattices exhibit, at higher temperatures, orientationally disordered phases. Such a disorder often involves pseudosymmetry, with the molecules constituting the crystal occupying lattice sites of symmetry higher than their own. Usually, on cooling, these phases undergo one or several transitions to more ordered phases with a corresponding loss of entropy. Examples are azulene[1] and dimethylnaphthalene,[2] in which the non-centrosymmetric molecules occupy lattice sites with inversion symmetry. A more complicated and, in many respects unique, case is that of acenaphthylene, $C_{12}H_8$ (henceforth referred to as ACNA).[3–9]

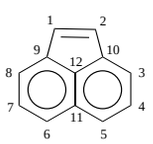

⟨ACNA⟩

X-Ray,[4] neutron diffraction[5] and more recent calorimetric[6] studies show that ACNA has three solid phases. What makes it exceptional, however, is the fact that all of these phases are highly disordered. Earlier ^{1}H NMR linewidth[7] and relaxation[8] measurements indicate that the disorder is dynamic on the NMR timescale with the molecules undergoing several types of motions. However, no definitive assignment of these motions to particular sites in the crystal was possible at the time. Since these early NMR studies, additional information on the structure of the various solid phases was acquired using neutron diffraction,[5] semi-empirical potential energy calculations[9] and thermophysical measurements.[6] We therefore decided to reinvestigate this system by ^{2}H NMR analysis of deuteriated ACNA. There are several advantages of using ^{2}H NMR spectroscopy in such studies: the deuterium spectral lineshape and relaxation are predominantly determined by the quadrupole coupling interaction whose magnitude and orientation in the molecular frame are well defined and therefore allow for a more detailed analysis of the experimental results. Also, due to spin diffusion effects ^{1}H NMR spectroscopy exhibits average properties over the various crystallographic species, while in ^{2}H NMR spectroscopy, where this effect is usually unimportant, different species exhibit different lineshapes and different relaxation behaviour, which can be analysed separately.

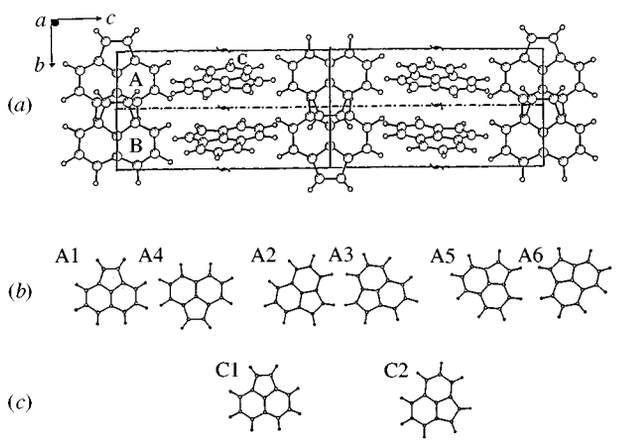

Fig. 1 (*a*) One of the possible configurations of the ACNA unit cell in Phase III as determined[5] by neutron diffraction: a projection down the *a* axis. The crystallographic average space group is $P2_1nm$ with $a = 7.585$ Å, $b = 7.590$ Å and $c = 27.851$ Å. There are eight molecules in the unit cell with three distinct crystallographic sites, A, B and C as indicated. All other sites are related to these by the symmetry elements of $P2_1nm$. Site B is ordered but the molecules in sites A and C are, respectively, six- and two-fold disordered as shown in (*b*) and (*c*). The notation used is that of ref. 5.

The earlier X-ray diffraction studies of Welberry[4] indicate the occurrence of a broad solid–solid transition at *ca.* 130 K with an intermediate phase in the transition region. The more recent calorimetric investigation by Cheda and Westrum[6] clearly showed the presence of three solid phases with the following sequence.

$$\text{Phase III} \xrightarrow[0.79\ \text{kJ mol}^{-1}]{116.6\ \text{K}} \text{Phase II} \xrightarrow[0.66\ \text{kJ mol}^{-1}]{127.1\ \text{K}} \text{Phase I}$$

All three phases are orthorhombic (in fact, pseudo-tetragonal with $a \approx b < c$) and consist of alternate 'herring bone' type layers of molecules along the (long) *c* axis. In the low temperature phase (Phase III) the layer repeat is of order four (space group $P2_1nm$ with 8 molecules per unit cell) as illustrated in Fig. 1(*a*). In the first layer the molecules are nearly parallel to the *bc* plane, with molecules A and B tilted alternatively by *ca.* 20° above and below the plane. In this phase, molecules A and B are crystallographically inequivalent. Site B is ordered, while

site A is disordered, with six different molecular orientations related by rotations in the molecular plane [see Fig. 1(*b*)]. The next layer consists of molecules (C) which are nearly parallel to the *ac* plane, tilted alternately by *ca.* 20° above and below this plane. The C sites are also disordered with two orientations related by rotation in the molecular plane [Fig. 1(*c*)]. The third and fourth layer in the unit cell are related to the first two layers by symmetry elements of the $P2_1nm$ space group. The high temperature phase (Phase I) has the same layer structure as Phase III but now sites A and B are equivalent and all sites, (A,B) and C, are disordered. The unit cell in Phase I is halved with just four molecules, two of type (A,B) and two of type C, resulting in a layer repeat of order two. The crystal structure corresponds to an average space group *Pbam* (or *Pba*2) although 'with the disorder present the concept of a space group is not really applicable'[4] anymore. The intermediate phase (Phase II) is much less understood. It also exhibits the (A,B)–(C)–repeat, but apparently with a six layer sequence.[4]

It is perhaps not surprising that ACNA exhibits such a variety of orientationally disordered structures. Although the molecule has only C_{2v} symmetry, shape-wise it is nearly trigonal with a pseudo-three-fold axis perpendicular to the molecular plane. On a coarser resolution it may even be considered as a disc with an irregular periphery. The calorimetric studies[6] indicate that the transition between the solid phases are quite sluggish leading to undercooling and trapping of more or less disorder, depending on the cooling rate.

The ^{1}H NMR measurements of Sanford *et al.*[8] suggest the occurrence of molecular motions already in Phase III. The transition to the high temperature phases involves a discontinuous increase in the rate of these motions. The proton T_1 measurements in Phase I exhibit two minima which implies that there are at least two types of motions, but as indicated above, they do not allow for an unequivocal identification of their nature.

The present ^{2}H NMR study concerns mainly Phase I. In Phase III the molecular motion is too slow to affect the spectral lineshape, while in Phase II the dynamic effects are not sufficient for a detailed kinetic analysis. The results in Phase I are much more conclusive. Both, the lineshape and the T_1 measurements, clearly indicate the occurrence of just two types of motions which could be quantitatively analysed in terms of reorientation within the molecular plane. We argue that the two motions correspond to the molecules in the A,B and C layers, respectively.

Experimental

Preparation of compounds

Three deuteriated isotopomers of ACNA were prepared: (*i*) perdeuteriated ACNA ([$^2H_8$]ACNA). (*ii*) ACNA deuteriated in the aromatic sites only ([$^2H_6$]ACNA). In this compound the deuteriation at C-4/7 is only 70%. (*iii*) ACNA specifically deuteriated at the olefinic C-1/2 ([$^2H_2$]ACNA). This compound also contains *ca.* 30% deuterium at C-4/7.

The deuteriated ACNAs were prepared by dehydrogenation of the corresponding deuteriated acenaphthene. In a typical experiment 9.1 g of *N*-bromosuccinimide and a small amount of benzoylperoxide were added to a solution containing 3.9 g of the acenaphthene isotopomer in CCl_4.[10] The mixture was refluxed for 45 min and allowed to cool. After removing the solid succinimide, the solvent was evaporated yielding solid 1,2-dibromoacenaphthene, which was crystallized twice from benzene–ethanol (yield: 4.1 g). The dibromo compound so obtained was dissolved in 80 ml absolute ethanol and the solution added slowly, while stirring, to a mixture containing 21.5 g zinc powder in 100 ml absolute ethanol. The reaction mixture was refluxed for 2 h, allowed to cool and kept overnight to allow all the zinc salt to precipitate. The solution was subsequently decanted into 500 ml of 5% HCl, where upon standing yellow crystals of ACNA developed. The crystals were filtered, air dried and sublimed three times under reduced pressure at 50 °C, yielding 0.8 g of pure ACNA. The resulting compound had the same isotopic composition as that of the acenaphthene precursors.

The various deuteriated acenaphthene precursors were prepared by the following method. Perdeuteriated acenaphthene ($C_{12}D_{10}$) was obtained from the undeuteriated compound (Aldrich $C_{12}H_{10}$) by exchange; 3 g of $C_{12}H_{10}$ were mixed with 40 ml D_2O and 500 mg Pt/C (10%) in a 100 ml autoclave. The mixture was heated to 220 °C while stirring for 5 days. After cooling, the crystalline product was filtered and sublimed yielding [$^2H_{10}$]acenaphthene with 96–98% deuteriation.

To prepare selectively deuteriated acenaphthene we employed the High Dilution High Temperature (HDHT) method[11,12] (exchange in 4% DCl–D_2O at 160 °C for 48 h in a tantalum autoclave). Under these conditions only the aromatic hydrogens exchange, while those of the methylene group remain unaffected. In practice the hydrogen exchange in positions 3/8 and 5/6 is complete but at positions 4/7 it is only partial (70%). This isotopomer of acenaphthene was used to prepare ACNA specifically deuteriated in the aromatic sites ([$^2H_6$]ACNA). Applying the HDHT method to perdeuteriated acenaphthene with HCl–H_2O yielded acenaphthene fully deuteriated at the methylene hydrogens and partially deuteriated (30%) at C-4/7. This isotopomer served as a precursor for the ACNA deuteriated in the olefinic carbons ([$^2H_2$]ACNA).

NMR measurements

^{2}H NMR measurements of powder ACNA samples were performed at 46.07 MHz on a high power Bruker CXP300 spectrometer controlled by a Tecmag MacSpect. The spectra were acquired by the quadrupole echo sequence $\pi/2 - t - \pi/2 - t -$ acquisition, with phase alternation, using $t = 15$ μs. The $\pi/2$ pulse length was 2.5 μs. Longitudinal relaxation times were measured by inversion recovery using composite π-pulses[13] to invert the magnetization and the signal was detected by a quadrupole echo sequence, followed by Fourier transformation. The quantitative analysis of the time evolution of the magnetization, $M(t)$ was carried out for features in the powder spectrum which exhibited just two decays. These were interpreted in terms of a biexponential function $M(t) = M(\infty)\{1 - \kappa[\exp(-t/T_1^1) + \exp(-t/T_1^2)]\}$ where the parameter κ (rather than 1) accounts for the incomplete inversion of the magnetization. The temperature was controlled by a Bruker VT1000 unit and independently monitored with an external thermocouple.

Computation of the dynamic lineshapes

The computation of the dynamic lineshapes were carried out as described in ref. 14, using the time interval between the quadrupole echo pulses of $t = 15$ μs. For the calculations of the site frequencies, ν_i, in the molecular frame we used the relation in eqn. (1) where $\nu_1 = 3e^2qQ/4h$ is the major principal component

$$\nu_i = \nu_1 \sin^2\beta\cos^2(\alpha + \gamma_i) + \nu_2 \sin^2\beta\sin^2(\alpha + \gamma_i) + \nu_3\cos^2\beta \quad (1)$$

of the deuterium quadrupole coupling interaction assumed to be along the C–D_i bond, ν_3 is the principal component perpendicular to the molecular plane and α,β are the polar angles of the magnetic field in this frame, with Z along the perpendicular to the molecular plane and γ_i the azimuthal orientation of the C–D_i bond. For the calculation of the dynamic spectra we assumed an axially symmetric quadrupole coupling $\nu_2 = \nu_3 = -\frac{1}{2}\nu_1 = -\frac{1}{2}\nu_q$ so that eqn. (1) reduces to eqn. (2). Powder

$$\nu_i = \tfrac{1}{2}\nu_q[3\cos^2(\alpha + \gamma_i)\sin^2\beta - 1] \quad (2)$$

spectra where calculated by integration over 6044 α,β pairs

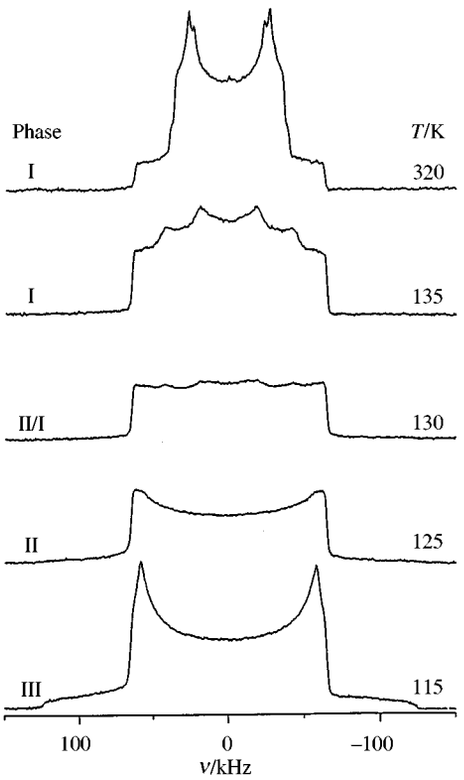

Fig. 2 ^{2}H NMR spectra (at 46.07 MHz) of a powder sample of [$^2H_6$]ACNA in the various solid phases at the indicated temperatures. The spectra were obtained by the quadrupole echo sequence, with a time interval of 15 μs between pulses.

using Conroy's sampling algorithm[15] and an exchange independent linewidth $1/T_2^0 = 5000\ s^{-1}$.

Results and discussion

Deuterium powder spectra in the various solid phases of ACNA

Examples of ^{2}H NMR spectra of perdeuteriated [$^2H_6$]ACNA in the various solid phases are shown in Fig. 2. The spectrum in Phase III (115 K) is typical of a rigid powder. It corresponds to a quadrupole coupling interaction of $3e^2qQ/4h = 128$ kHz and an asymmetry parameter $\eta = 0.05$. We conclude that in this phase any molecular reorientation is slower than the natural deuterium linewidth ($1/T_2^0 \sim 10^4\ s^{-1}$ and probably much slower). Heating to above the Phase III/Phase II transition results in a discontinuous change in the lineshape due to the onset of molecular motion (see trace at 125 K): the 'parallel' shoulders flatten, the 'perpendicular' features round off and there is an increase in the relative intensity at the centre part of the spectrum. This spectrum corresponds to reorientation rates of *ca.* 10^4–$10^5\ s^{-1}$. However, the lineshape does not exhibit sufficient characteristic features to allow a detailed analysis, in particular, since from the crystal structure we anticipate a complex situation with at least two different dynamic species. Also, because of the sluggish solid–solid phase transitions, the spectra in the region 120–130 K possibly correspond to a superposition of signals due to Phase II and Phase I (see the 130 K trace in Fig. 2).

At about 130 K there is another change in the spectrum which then evolves continuously as a function of temperature within the Phase I region. The temperature dependence of the spectrum is now completely reversible and, as described in the next section, it corresponds to a 1:1 superposition of two dynamically averaged subspectra, which we indicate as **1** and **2**.

Dynamic lineshape in phase I

A more detailed description of the evolution of the NMR spectra with temperature, within Phase I, is shown in Fig. 3(*a*).

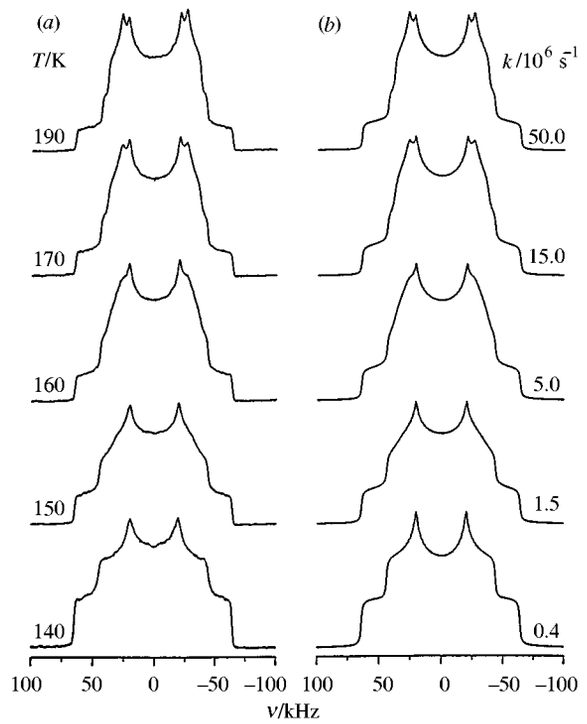

Fig. 3 (*a*) Experimental ^{2}H NMR spectra of [$^2H_6$]ACNA in Phase I. Experimental details as in Fig. 2. (*b*) Simulated spectra calculated as described in the text. The traces correspond to a superposition of two subspectra (**1** and **2**) with relative intensity 1:1. Spectrum **1** is a fast exchange biaxial spectrum with average quadrupole coupling parameters $\langle \nu_q^1 \rangle = 64$ kHz, and asymmetry parameters obtained by extrapolation of the η^1 curve of Fig. 4. Spectrum **2** is a dynamic three-fold jump spectrum in a Y-geometry with $\varepsilon = 3.0°$ and three axially symmetric congruent quadrupole coupling splitting parameters $\nu_q^2 = 128$ kHz, at the indicated jump rate constants. An effective linewidth parameter $1/T_2^0 = 5000\ s^{-1}$ was used in the calculations.

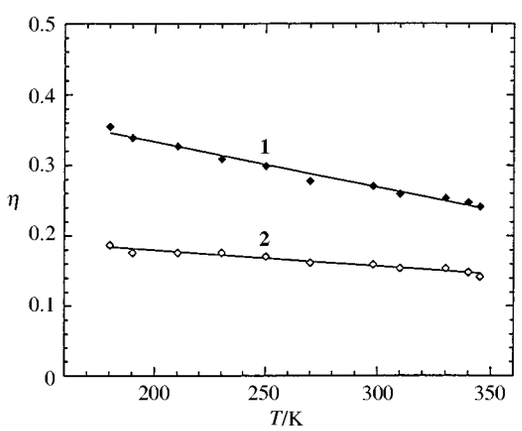

Fig. 4 Plots of the spectral asymmetry parameters η^1 and η^2 for the two deuterium subspectra in the high temperature Phase I of ACNA as a function of temperature

The gradual change in the lineshape leads at temperatures above 170 K to a pattern which can readily be interpreted in terms of a 1:1 superposition of two biaxial powder spectra with average quadrupole coupling parameters (at 200 K) of $\langle \nu_q^1 \rangle = \langle \nu_q^2 \rangle = 64$ kHz, $\eta^1 = 0.355$ and $\eta^2 = 0.181$. Note that the $\langle \nu_q^i \rangle$ values are essentially half the value of ν_q in the static spectrum of Phase III. They are fairly constant within the entire range of Phase I, but the values of η^1 and η^2 change slightly as a function of temperature. This dependence is plotted in Fig. 4 in the temperature range where the η^i values could be determined accurately (>170 K). In this temperature range $\langle \nu_q \rangle$ reduces by *ca.* 1 kHz, from 64 at 170 K to 63 kHz at 350 K.

The spectra shown in Figs. 2 and 3 correspond to [$^2H_6$]ACNA

which contains a number of non-equivalent aromatic deuterons. Identical spectra were also observed for the [$^2H_2$]ACNA and [$^2H_8$]ACNA isotopomers (see Experimental section), indicating that within the experimental resolution, all ACNA deuterons exhibit identical powder lineshapes over the entire temperature range of the solid phases. This means that whatever dynamic processes are responsible for the changes in the deuterium lineshape they can only involve planar reorientation about the pseudo-three-fold axis of the ACNA molecule. Any out-of-plane flips would render the various types of deuterons significantly inequivalent and result in a much more complex lineshape than experimentally observed. The fact that the overall average width of both subspectra in Phase I is reduced to one half its value in the static spectrum of Phase III is also consistent with this conclusion. Whether these processes correspond to two- or higher-fold jumps can only be determined by a detailed analysis of the experimental dynamic lineshapes.

A variety of preliminary simulations using the procedure outlined in the Experimental section convinced us that one of the subspectra, *i.e.* the one indicated by **1** in Fig. 4, already corresponds to the fast exchange regime at the Phase II to Phase I transition. We therefore fixed its lineshape by extrapolation of the η^1 curve to the dynamic region. To simulate the dynamic spectra of species **2** we first note that an average biaxial spectrum can be obtained by assuming (*i*) symmetric *n*-fold jumps (by $2\pi/n$) with unequal populations in the various orientations, (*ii*) non-symmetric *n*-fold jumps with equal population or (*iii*) a combination of both non-symmetric jumps (with jump angles different from $2\pi n$) with differently populated orientations. Since, however, the temperature dependence of η^2 is quite small and in order to simplify the analysis we assumed that the dynamic process involves jumps between non-symmetric orientations, but with equal fractional populations, $P_i = 1/n$. The jump angles can then be fixed by requiring that in the fast exchange limit the observed average quadrupole coupling tensor, $\langle Q \rangle$, is the weighted average of the static tensors, Q_i, in their respective orientations [eqn. (3)]. We assume that the tensors

$$\langle Q \rangle = \sum_i P_i Q_i \qquad (3)$$

Q_i are congruent (*i.e.* have identical principal coupling constants) and that for all of them one of the minor components is perpendicular to the molecular plane. This principal value will remain unaffected by the reorientation motion. For simplicity we also assume that the Q_i values are axially symmetric with the unique component $\nu_q = 128$ kHz.

For a two-site jump ($n = 2$) the jump angle, θ, is uniquely determined (modulus π) by the experimental asymmetry parameter given in eqn. (4). Using θ values (~86°) derived from

$$\eta = 3 \cos \theta \qquad (4)$$

this equation with the η^2 curve of Fig. 4 we attempted to simulate the results of Fig. 3. However, except for the very fast jump limit, no reasonable fit with the experimental spectra (after adding the spectrum of species **1**) could be obtained. We thus rule out a two-site jump model for species **2** and proceed to higher-fold planar jumps. For three sites with equal fractional populations $P_i = 1/3$, the asymmetry parameter of the average tensor depends on two angles, *e.g.* θ_{12} and θ_{23} (with $\theta_{31} = 2\pi - \theta_{12} - \theta_{23}$) where $\theta_{ij} = \gamma_i - \gamma_j$ is the jump angle between orientations *i* and *j*. Rather than fitting the dynamic spectra to two θ_{ij} values we assumed that $\theta_{12} = \theta_{23} = 120 - \varepsilon$ and $\theta_{31} = 120 + 2\varepsilon$, which corresponds to a Y-shaped tripod. For this geometry the relation between ε and η is given in eqn. (5) where for small ε

$$\cos 2\left(\frac{2\pi}{3} - \varepsilon\right) = -\tfrac{1}{2}(1 + \eta) \qquad (5)$$

one needs to choose the third quadrant for the $2(2\pi/3 - \varepsilon)$ angle. From Fig. 4 with $\eta^2 = 0.18$ an average value of $\varepsilon = 3.0°$ may be derived. Thus the deviation from perfect three-fold symmetry is indeed quite small. With this model we were able to obtain a very satisfactory fit with the experimental spectra as shown by the simulations on the right hand side of Fig. 3. It should, however, be noted that identical simulated spectra are obtained for a six-fold jump model in which three additional orientations at $\gamma_{i+3} = \gamma_i + \pi$ are added to the Y-model, assuming nearest neighbour jumps. In fact we could also simulate the experimental spectra using four- and eight-fold jumps with appropriate distortion from regular symmetry (to fit the experimental η values). We thus conclude that the molecular dynamics in site **2** involves planar three- or higher-fold jumps, but without further information we cannot choose between the various models.

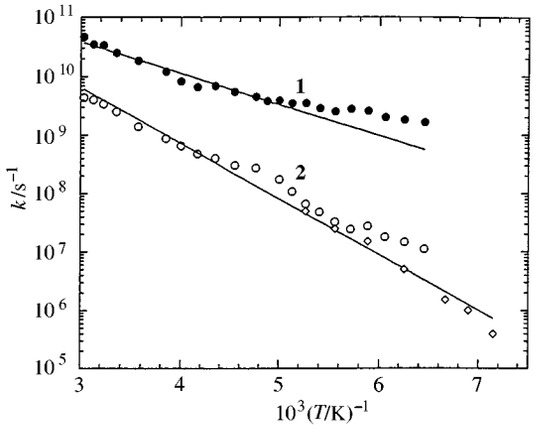

Fig. 5 Arrhenius plots for the rate constants of the planar reorientations in the two ACNA species of Phase I. The calculations assume three-fold jumps for both sites. (◇), results from the lineshape analysis; (○, ●), results from T_1 relaxation measurements. The solid lines are calculated using the parameters of Table 1.

Assuming the three-fold jump model, the best fit values for the jump rates, k_2, in site **2** are plotted as a function of the inverse absolute temperature in Fig. 5.

Relaxation measurements

To extend the kinetic studies of species **2** and gain more information about the dynamics of species **1**, we have measured the deuterium longitudinal relaxation time, T_1, in the deuteriated ACNA sample over a wide temperature range. Quite long relaxation times were measured in Phase III, which shortened significantly in the transition range to Phase II and I due to the onset of fast molecular motions. We will again restrict the quantitative analysis of the measurements to the high temperature Phase I.

Theoretical expressions for the deuterium T_1 relaxation due to various planar reorientations has been given by Torchia and Szabo.[16] For such motions T_1 is anisotropic and therefore the relaxation decay of a powder spectrum should be multi-exponential and difficult to analyse. The analysis may be simplified by considering spectral regions which correspond to specific, or at least a narrow range of orientations of the magnetic field with respect to the molecular frame. In the fast exchange limit ($2\pi\nu_q\tau < 1$, where τ is the correlation time for the motion) the outer shoulders of the average deuterium spectrum provide such spectral regions. These shoulders correspond to molecules whose pseudo-three-fold axes lie parallel to the external magnetic field, B_0 ($\theta = 0°$ in the notation of ref. 16), while the major principal component of the deuterium quadrupole tensor is perpendicular to B_0 ($\theta = \pi/2$). The signal at these shoulders should therefore decay biexponentially, one decay for each of the species **1** and **2**, with equal initial intensities. This was indeed observed experimentally and the results for the two T_1 values (derived as explained in the Experimental

Table 1 Arrhenius activation parameters in the two sites of ACNA[a]

	ΔE_1/kJ mol^{-1}	$k_1^0/10^{12}$ s^{-1}	k_1(300 K)/10^{10} s^{-1}	ΔE_2/kJ mol^{-1}	$k_2^0/10^{12}$ s^{-1}	k_2(300 K)/10^9 s^{-1}
Present work	10.2	1.5	2.6	18.3	4.8	3.1
Sanford *et al.*[8]	14.2	51	17	18.9	4.7	2.4

[a] $k_i = 1/(3\tau_i) = k_i^0 \exp(-\Delta E_i/RT)$.

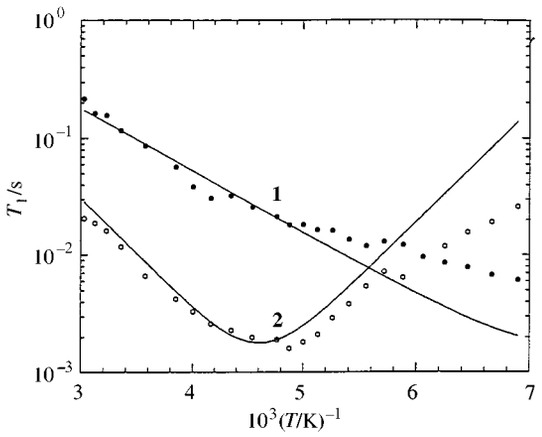

Fig. 6 Plots of the two T_1 values as measured from the inversion recovery of the outer shoulders of the deuterium powder spectrum in Phase I. The solid curves are calculated using eqn. (6) and the kinetic parameters of Table 1.

section) are plotted as a function of the reciprocal absolute temperature in Fig. 6. The two T_1 values exhibit a quite different temperature dependence: while the T_1 values of one component increase monotonically with increasing temperature, as would be expected for the extreme fast exchange regime ($\omega_0\tau \ll 1$), the T_1 values of the second component pass through a minimum ($\omega_0\tau \sim 1$). Clearly the former corresponds to species **1**, while the latter may be identified with species **2**.

Assuming three-fold jumps for species **2** and neglecting the small deviation from trigonal symmetry, T_1 can be expressed by eqn. (6), where $\tau_2 = 1/(3k_2)$ and k_2 is the rate constant for jumps

$$\frac{1}{T_1^2} = (2\pi\nu_q)^2 \frac{\tau_2}{1 + 4(\omega_0\tau_2)^2} \qquad (6)$$

between the different orientations of species **2**. The k_2 values obtained by best fitting the experimental relaxation results to eqn. (6) are plotted in Fig. 5 together with those derived from the lineshape analysis. The resulting Arrhenius parameters are summarized in Table 1.

We have also used eqn. (6) to analyse the T_1 data in species **1**, which in the extreme fast motion reduces to $1/T_1^1 = (2\pi\nu_Q)^2\tau_1$. The results so obtained are included in Table 1 and in Fig. 5. The full lines in Figs. 5 and 6 are calculated using these Arrhenius parameters. The fit of the two sets of data is quite reasonable. Deviation in the T_1 fit are observed at low temperatures where $2\pi\nu_q\tau \geqslant 1$. In this range the assumption that the shoulders at $\pm\langle\nu_q\rangle$ comprise just two contributions does not apply anymore and the analysis of the magnetization decay in terms of a biexponential function is not strictly justified.

Conclusions

The results of the present work are consistent with the earlier ^{1}H NMR measurements on ACNA (see Table 1) and provide more definitive interpretation for the two types of motions which were also observed in these studies.[8] From the powder spectra it is, however, not possible to associate the kinetic parameters to particular sites in the crystal structure. Such an assignment would have been possible if the measurements were carried out on oriented single crystals. Unfortunately, our attempts to grow single crystals, suitable for NMR measurements, either from the melt or from solution, failed. We can therefore only speculate on the most likely assignment.

A clue for the assignment may be provided by the neutron structure[5] and the potential energy calculations[9] of the low temperature Phase III. In this phase it was found that site B is ordered with the projection of the C(11)–C(12) direction (henceforth referred to as the molecular orientation) at 0° and 180° relative to the *b* crystallographic axis [see Fig. 1(*a*)], while site A is disordered with six different unequally populated orientations at approximately (0°, 180°), (45°, 225°) and (135°, 315°) (where the pairs in brackets are magnetically equivalent orientations) as shown in Fig. 1(*b*). For site C, which is also disordered, two orientations [Fig. 1(*c*)] at approximately 0° and 120° relative to the crystallographic *a* axis (and two additional symmetry related sites) could be located by the refinement procedure used.[5] It is readily seen that the projections of the six orientations of site A or the two orientations of site C trace similar profiles. The semi-empirical calculations of He and Welberry[9] show that the potential energies of the 12 configurations (six possible A orientations times two possible C orientations) are quite close. In fact, 10 configurations are within 2.5 kJ mol^{-1} of the most stable one and two are *ca.* 10 kJ mol^{-1} higher. The neutron diffraction results[5] show that all six orientations of A and the two orientations of C are significantly populated in the low temperature phase, although not to the same extent; the 0° orientation of A (A^1) constitutes *ca.* 55% and each of the others *ca.* 9%, while the population ratio of the two C sites is *ca.* 2.4:1. Before the neutron structure of the low temperature phase (Phase III) was published,[5] Sanford *et al.*[8] attempted to calculate the energy barrier to rotation in the various crystal sites, using crystal parameters of the earlier, less accurate, X-ray structure.[4] It is nevertheless instructive to refer to their results in connection with the present work. For all sites they find a multitude of potential minima, but many more (eight) and considerably deeper (40–60 kJ mol^{-1}) for the A,B sites and a much shallower (~20 kJ mol^{-1}) potential, with just three minima for the C sites. These estimates will no doubt change when the newly determined structure[5] is used for the calculations. However, the relative barrier heights for the two types of sites will probably remain.

We recall that Phase I has essentially the same layered structure as Phase III, but with two layer repeat, (A,B)–C–(A,B)–C . . . , in which the A,B molecules are equivalent but different from C. Also, the unit cell dimensions in Phase I are somewhat expanded relative to those in Phase III, thus reducing the intermolecular interaction. On the basis of these crystallographic and potential energy considerations it is most likely to associate our NMR species **1** and **2** with, respectively, the crystallographic sites C and (A,B). In the (A,B) site of Phase I there are a number of orientations (perhaps six or eight) with similar populations and nearly symmetrical arrangement. Consequently the spectra can be fitted to multiple planar jumps, leading in the fast exchange limit to a slightly biaxial spectrum with a weakly temperature dependent asymmetry parameter. In site C the molecules undergo much faster two- or higher-fold jumps between orientations possibly not equally populated even in Phase I. Hence the average spectrum exhibits a larger asymmetry which is more strongly temperature dependent than for the (A,B) molecules. From the fact that the kinetic parameters for the two sites differ significantly, we may also conclude

that the reorientational motions in adjacent layers are not correlated.

As indicated, more conclusive assignment of species **1** and **2** could be obtained if suitable single crystals were available or by more precise lattice dynamic calculations.

Acknowledgements

We thank Professor L. Leiserowitz for many helpful discussions of the acenaphthylene crystal structure. This research was supported by a grant from G. I. F. The German–Israeli Foundation for Scientific Research and Development.

References

1 N. Karl, H. Heym and J. J. Stezowski, *Mol. Cryst. Liq. Cryst.*, 1985, **131**, 163.
2 J. Robertson, H. M. M. Shearer, G. A. Sim and D. G. Warson, *Acta Crystallogr.*, 1962, **15**, 1.
3 M. D. Cohen, I. Ron, G. M. Schmidt and J. M. Thomas, *Nature*, 1969, **224**, 167; R. D. Gordon and R. F. Yang, *J. Mol. Spectrosc.*, 1970, **34**, 266; H. Gyula, G. Kovacs, F. Cser and G. Koszterszits, *Magy. Kem. Foly.*, 1971, **77**, 11.
4 T. R. Welberry, *Proc. R. Soc. London, Ser. A*, 1973, **334**, 19.
5 R. A. Wood, T. R. Welberry and A. D. Rae, *J. Chem. Soc., Perkin Trans. 2*, 1985, 451.
6 J. A. R. Cheda and E. F. Westrum, Jr., *J. Phys. Chem.*, 1994, **98**, 2482.
7 C. A. Fyfe and G. J. Kupferschmidt, *Mol. Cryst. Liq. Cryst.*, 1973, **28**, 179.
8 W. E. Sanford, G. J. Kupferschmidt, C. A. Fyfe, R. K. Boyd and J. A. Ripmeester, *Can. J. Chem.*, 1980, **58**, 906.
9 H. He and T. R. Welberry, *J. Chem. Soc., Perkin Trans. 2*, 1988, 1947.
10 A. G. Anderson and R. G. Anderson, *J. Am. Chem. Soc.*, 1955, **77**, 6610.
11 N. H. Wertiuk and T. Kadai, *Can. J. Chem.*, 1974, **52**, 2169.
12 H. Zimmerman, *Liq. Cryst.*, 1989, **6**, 591.
13 N. J. Heaton, R. R. Vold and R. L. Vold, *J. Magn. Reson.*, 1988, **77**, 572; D. P. Raleigh, E. T. Olejniczak and R. G. Griffin, *J. Magn. Reson.*, 1989, **81**, 455.
14 A. J. Vega and Z. Luz, *J. Chem. Phys.*, 1987, **86**, 1803.
15 H. Conroy, *J. Chem. Phys.*, 1967, **47**, 5307; V. B. Cheng, H. H. Suzukawa and M. Wolfsberg, *J. Chem. Phys.*, 1973, **59**, 3992.
16 D. A. Torchia and A. Szabo, *J. Magn. Reson.*, 1982, **49**, 107.

Paper 7/00503B
Received 21*st January* 1997
Accepted 18*th March* 1997